The binormal flow, the Talbot effect, and non-circular jets

Luis VEGA, BCAM-UPV/EHU

(with V. Banica and F. De la Hoz)

basque center for applied mathematics

eman ta zabal zazu

NTNU, June 4th, 2019

HADE

Summary

(A) Binormal Flow **(BF)** a dispersive (geometric) PDE

- Critical regularity: Polygonal lines
- Selfsimilar solutions have finite energy $\left(\widehat{L^2}_{\text{per}}\right)$
- Talbot effect
- Continuation beyond the singularity time

(B) **BF** as a toy model in Fluid Mechanics: Vortex filament equation **(VFE)**

- Coherent structures are the self similar solutions
- Interaction: A weakly non–linear Talbot effect **(NLTe)**

Conjecture: **NLTe** can explain the turbulent dynamics of non circular jets

Q: **BF** for regular Polygons and regular polygonal helices

Annu. Rev. Fluid Mech. 1999. 31:239–72

FLOW CONTROL WITH NONCIRCULAR JETS[1]

E. J. Gutmark
Mechanical Engineering Department, Louisiana State University, Baton Rouge, Louisiana 70803-6413; e-mail: gutmark@me.lsu.edu

F. F. Grinstein
Laboratory for Computational Physics and Fluid Dynamics, Code 6410, Naval Research Laboratory, Washington, DC 20375-5344;
e-mail: grinstei@lcp.nrl.navy.mil

KEY WORDS: vortices, mixing, combustion, entrainment

ABSTRACT

Noncircular jets have been the topic of extensive research in the last fifteen years. These jets were identified as an efficient technique of passive flow control that allows significant improvements of performance in various practical systems at a relatively low cost because noncircular jets rely solely on changes in the geometry of the nozzle. The applications of noncircular jets discussed in this review include improved large- and small-scale mixing in low- and high-speed flows, and enhanced combustor performance, by improving combustion efficiency, reducing combustion instabilities and undesired emissions. Additional applications include noise suppression, heat transfer, and thrust vector control (TVC).

The flow patterns associated with noncircular jets involve mechanisms of vortex evolution and interaction, flow instabilities, and fine-scale turbulence augmentation. Stability theory identified the effects of initial momentum thickness distribution, aspect ratio, and radius of curvature on the initial flow evolution. Experiments revealed complex vortex evolution and interaction related to self-induction and interaction between azimuthal and axial vortices, which lead to axis switching in the mean flow field. Numerical simulations described the details and clarified mechanisms of vorticity dynamics and effects of heat release and reaction on noncircular jet behavior.

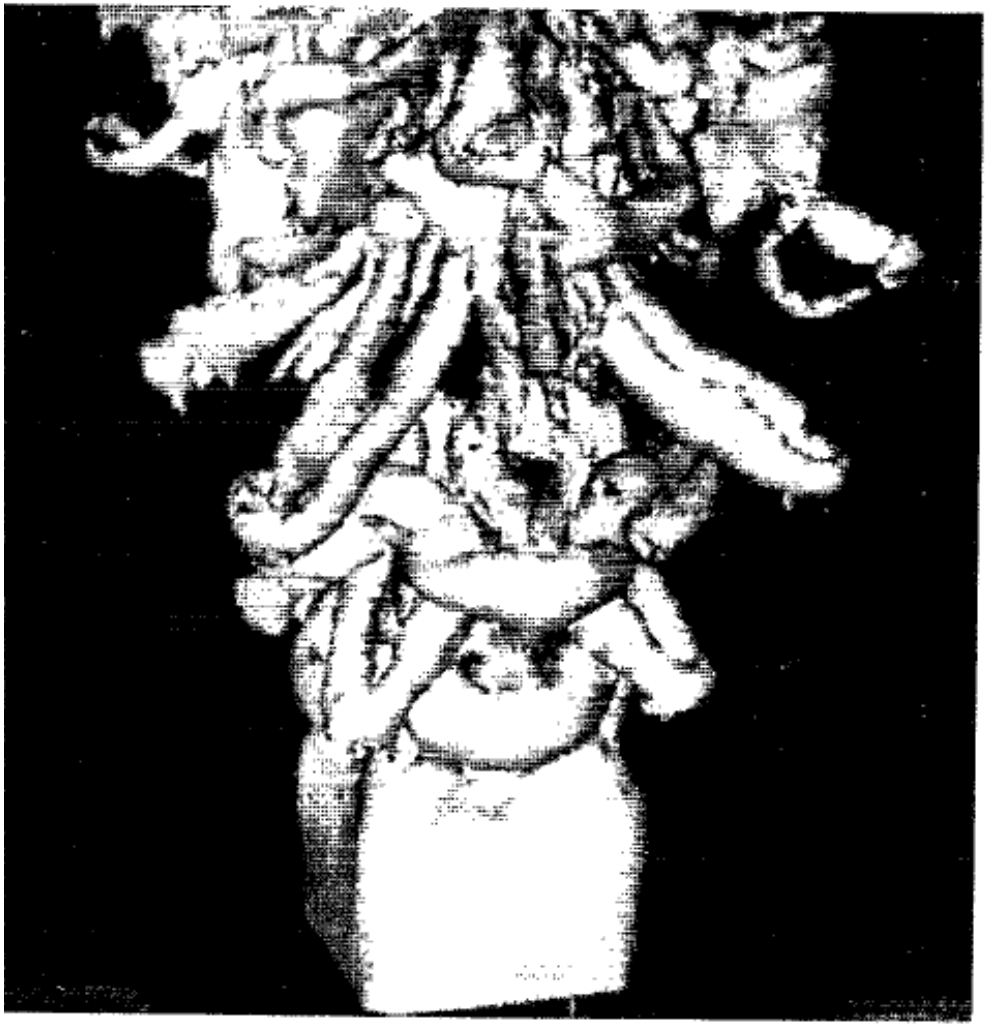

I, III, V : hairpin (braid) vortices
II, IV : deformed vortex rings

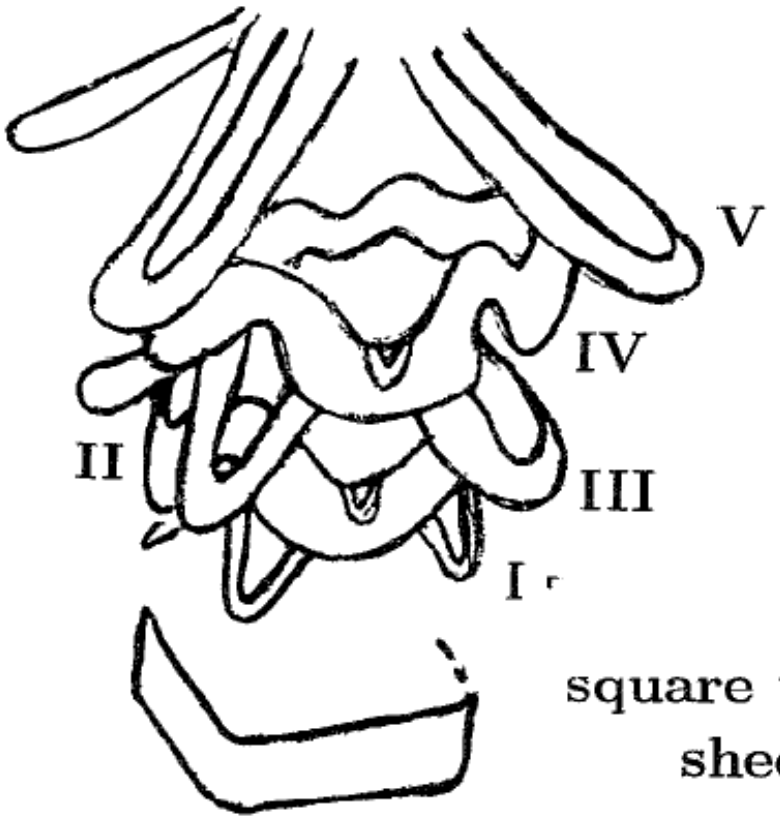

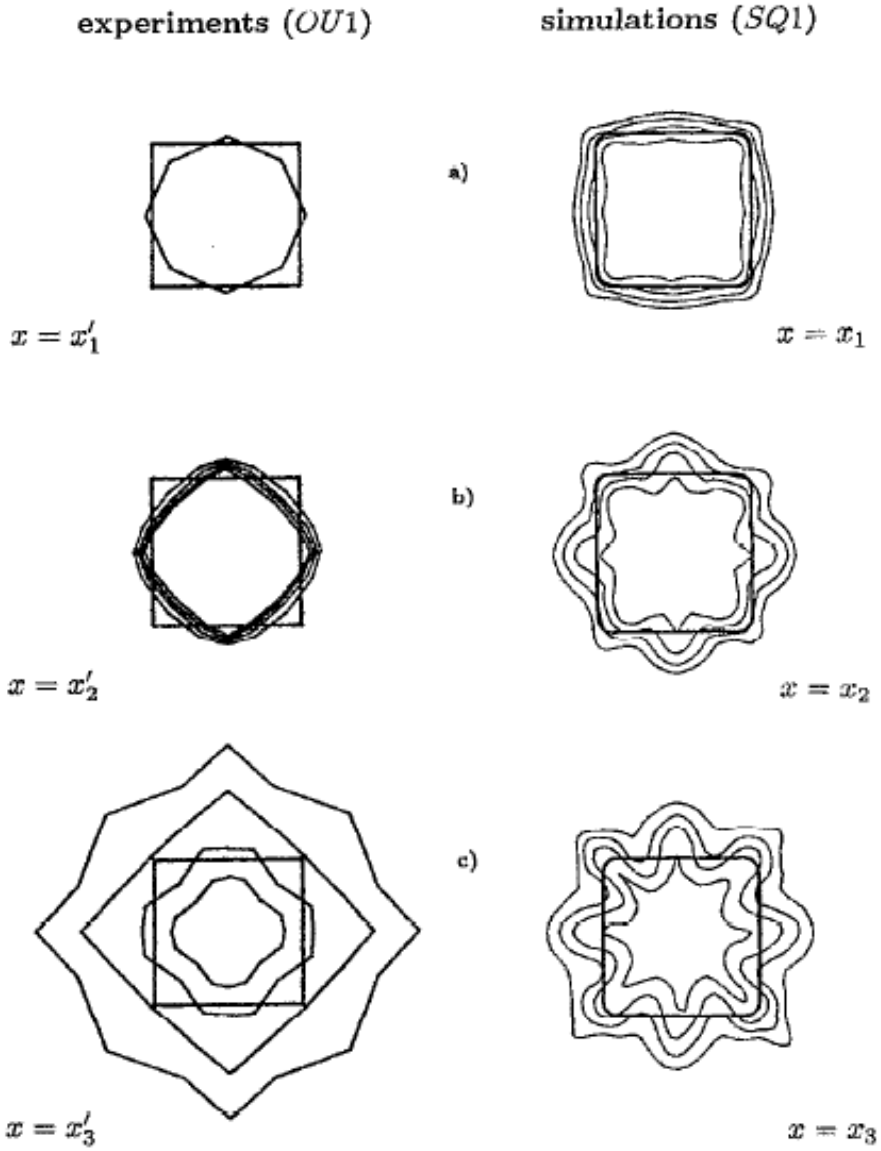

FIG. 10. Axis switching of the jet cross section in terms of isocontours of time-averaged streamwise velocity scaled with its local centerline value (u/u_{cl}) for experimental (OU1) and simulated (SQ1) jets. Contour levels are 0.2, 0.4, 0.6, and 0.8. The geometry of the experimental nozzle is superimposed on each slice on the left; the initial half-width velocity cross section of the simulated jets is superimposed on each slice on the right. The stream-

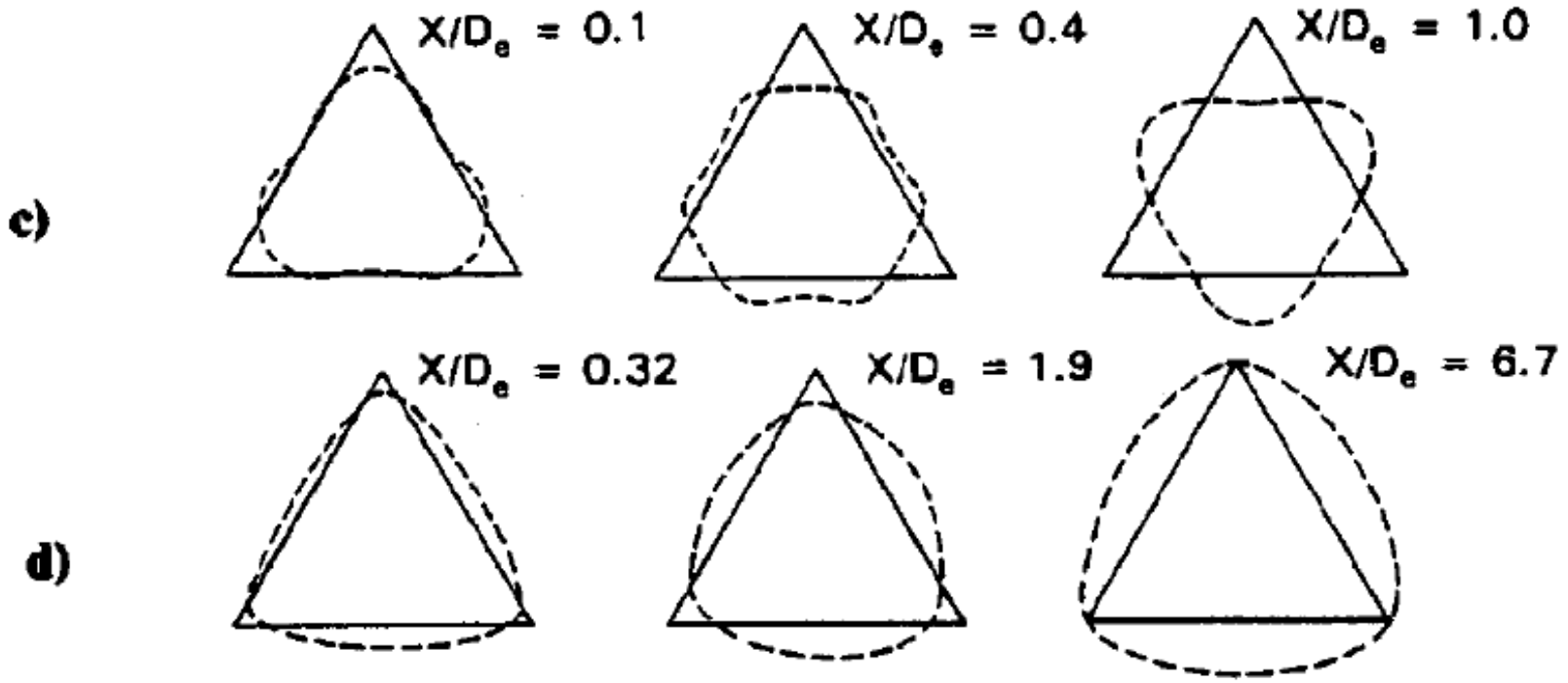

Figure 6 Variation of momentum thickness with axial distance at the vertex and flat sides of the triangular jet: (*a*) orifice jet, (*b*) pipe jet. Corresponding evolution of the jet cross-sections along the axis: (*c*) orifice jet, (*d*) pipe jet. (Koshigoe et al 1989)

Euler equations

u: velocity field

$\omega = \operatorname{curl} u = \nabla \wedge u$: vorticity

$\omega = \Gamma T ds \qquad T = X_s$

$X = X(s,t)$ curve in $\mathbb{R}^3$ support of ω

$\operatorname{div} u = 0$

$$u(P) = \frac{\Gamma}{4\pi} \int_{-\infty}^{\infty} \frac{X(s) - P}{|X(s) - P|^3} \wedge T(s) ds$$

Examples: straight lines, vortex rings, helical vortices

(A) Binormal Flow

(BF) • $\chi_t = \chi_s \wedge \chi_{ss} = cb$ $\quad c$: curvature $\quad b$: binormal

(SM) • $\chi_s = T$ Schrödinger map $\qquad T_t = T \wedge T_{ss}$

(NLS) • ψ Hashimoto wave function 1d **NLS** (cubic focusing)

$\chi(0,s)$: skew polygonal line

$T(0,s)$: sequence of points T_j such that $\lim_{j\to\pm\infty} T_j = A^{\pm}$

$$\psi(0,s) = \sum a_j \delta(s-j) \qquad \sum_j |j|^{1^+} |a_j|^2 < +\infty$$

$$\begin{pmatrix} T \\ e_1 \\ e_2 \end{pmatrix}_s = \begin{pmatrix} 0 & \alpha & \beta \\ -\alpha & 0 & 0 \\ -\beta & 0 & 0 \end{pmatrix} \begin{pmatrix} T \\ e_1 \\ e_2 \end{pmatrix}$$

$$\psi = \alpha + i\beta$$

(A) Binormal Flow

(BF) • $\chi_t = \chi_s \wedge \chi_{ss} = cb$ $\quad c$: curvature $\quad b$: binormal

(SM) • $\chi_s = T$ Schrödinger map $\qquad T_t = T \wedge T_{ss}$

(NLS) • ψ Hashimoto wave function 1d **NLS** (cubic focusing)

$\chi(0,s)$: skew polygonal line

$T(0,s)$: sequence of points T_j such that $\lim_{j\to\pm\infty} T_j = A^{\pm}$

$$\psi(0,s) = \sum a_j \delta(s-j) \qquad \sum_j |j|^{1^+} |a_j|^2 < +\infty$$

$$\begin{pmatrix} T \\ e_1 \\ e_2 \end{pmatrix}_s = \begin{pmatrix} 0 & \alpha & \beta \\ -\alpha & 0 & 0 \\ -\beta & 0 & 0 \end{pmatrix} \begin{pmatrix} T \\ n \\ b \end{pmatrix}$$

$$\psi = \alpha + i\beta$$

SCHRÖDINGER EQUATION

Hasimoto transformation:

$$\psi(s,t) = c(s,t)e^{i\int_0^s \tau(s',t)ds'}$$

$c = c(s,t)$ curvature

$\tau = \tau(s,t)$ torsion

$$\partial_t \psi(s,t) = i\left(\partial_s^2 \psi \pm \frac{1}{2}(|\psi|^2 + A(t))\psi\right)$$

$$\int_{-\infty}^{\infty} |\psi(s,t)|^2 ds = \int_{-\infty}^{\infty} |\psi(s,0)|^2 ds = \int_{-\infty}^{\infty} c^2(s,0) ds$$

In our case

$$\psi(s,t) = \frac{a}{\sqrt{t}} e^{i\frac{s^2}{4t}} \qquad , \qquad \int_{-\infty}^{\infty} |\psi|^2 ds = +\infty.$$

SOME HISTORY

What is the Talbot effect?

- Optical effect discovered by Talbot in 1836
- Describes the behaviour of light after passing through a grating

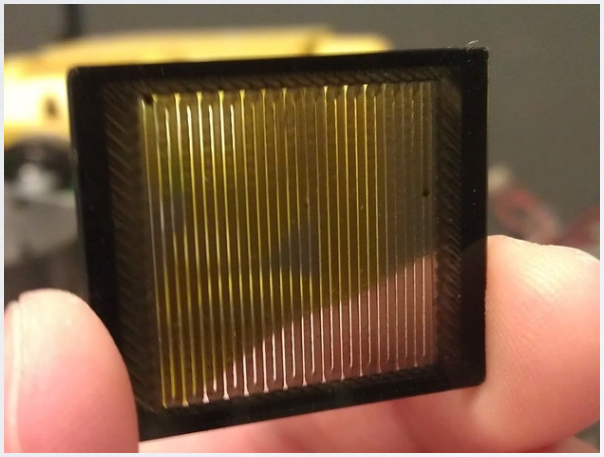

- Tight gratings: 6800 slits per centimetre! (Lord Rayleigh in 1879)

THE

LONDON AND EDINBURGH

PHILOSOPHICAL MAGAZINE

AND

JOURNAL OF SCIENCE.

[THIRD SERIES.]

DECEMBER 1836.

LXXVI. *Facts relating to Optical Science. No. IV.*
By H. F. TALBOT, *Esq., F.R.S.**

§ 1. *Experiments on the Interference of Light.*

ALTHOUGH so much has been explained in optical science by the aid of the undulatory hypothesis, yet when any *well-marked phænomena* occur which present unexpected peculiarities, it may be of importance to describe them, for the sake of comparison with the theory.

Such appears to me to be the case with those which I am about to mention, in which, by means of a remarkable compensation of some kind or other, common solar light appears to play the part of homogeneous light, and *to achromatize itself*, if I may use such an expression, in a very high degree of perfection.

Sir William Herschel was, I believe, the first who took notice of the very beautiful coloured bands which are seen by looking through two prisms placed in contact. Thus, let A B C, A D C be two equal right-angled glass prisms in contact. We will suppose the sides A B, B C to be equal, and the thickness of the prisms to be equal to A B, in which case the combination of the two will form a cube. Let the two prisms be gently pressed together by their face A C, which must be previously well cleaned from any adhering dust, and

* Communicated by the Author.

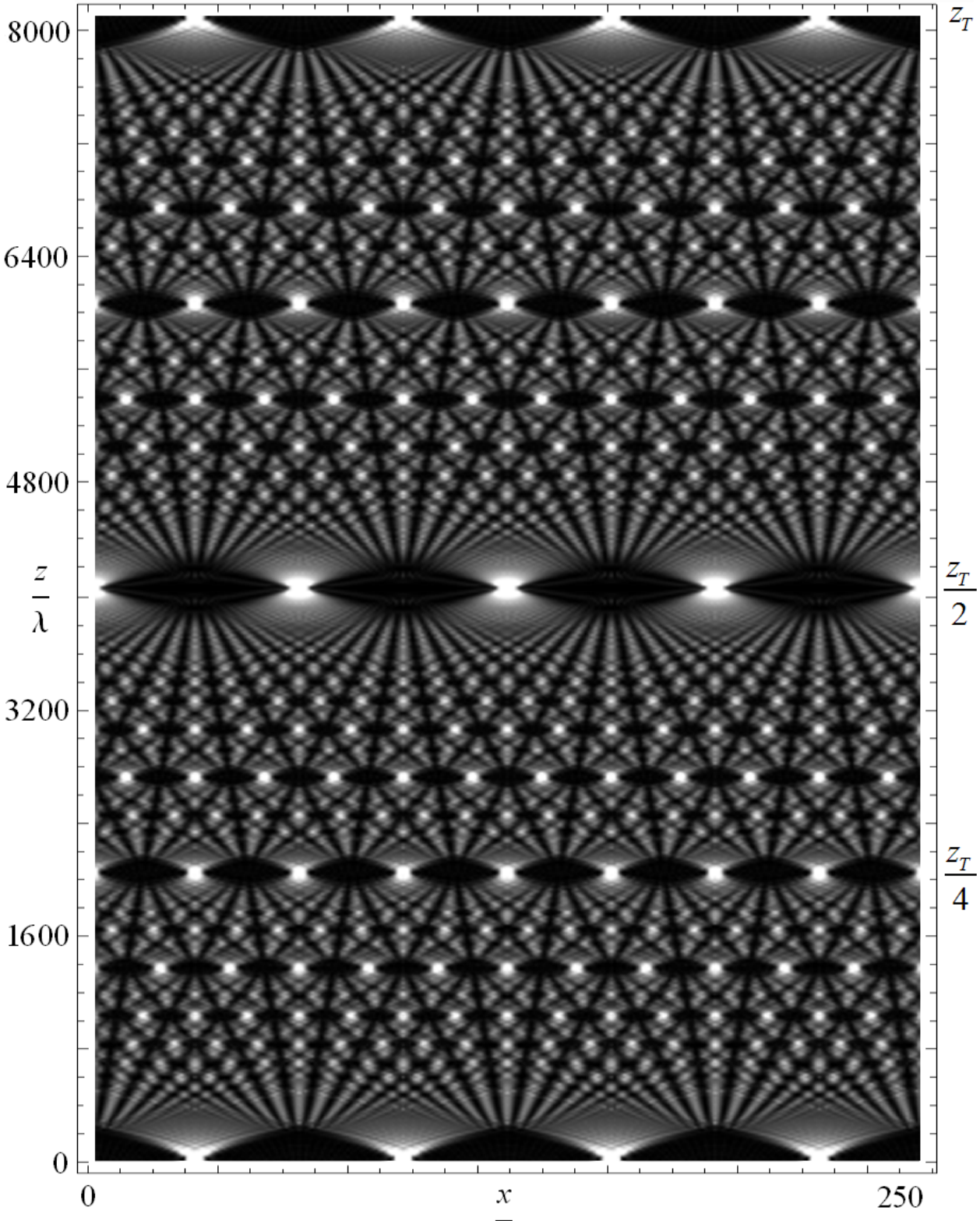
8000
6400
4800
3200
1600
0
$\frac{z}{\lambda}$
z_T
$\frac{z_T}{2}$
$\frac{z_T}{4}$
0
250
x

Talbot effect and linear Schrödinger equation

$$\psi_t \quad = \quad i\psi_{ss}$$

$$\psi(s,0) = \frac{2\pi}{M} \sum_{k=-\infty}^{\infty} \delta\left(s - \frac{2\pi k}{M}\right).$$

$$\widehat{\psi}(k,t) \quad = \quad e^{-i(Mk)^2 t}\widehat{\psi}(0,t)$$

$$t_{pq} = (2\pi/M^2)(p/q)$$

$$\begin{aligned}
\psi(s, t_{pq}) &= \sum_{k=-\infty}^{\infty} e^{-i(Mk)^2 2\pi p/(M^2 q) + iMks} \\
&= \sum_{k=-\infty}^{\infty} e^{-2\pi i(p/q)k^2 + iMks} \\
&= \sum_{l=0}^{q-1} \sum_{k=-\infty}^{\infty} e^{-2\pi i(p/q)(qk+l)^2 + iM(qk+l)s} \\
&= \sum_{l=0}^{q-1} e^{-2\pi i(p/q)l^2 + iMls} \sum_{k=-\infty}^{\infty} e^{iMqks}.
\end{aligned}$$

THE TALBOT EFFECT

$$t_{pq} = (2\pi/M^2)(p/q)$$

$$\psi(s,0) = \frac{2\pi}{M} \sum_{k=-\infty}^{\infty} \delta(s - \tfrac{2\pi k}{M}).$$

$$\psi(s,t_{pq}) = \frac{2\pi}{Mq} \sum_{k=-\infty}^{\infty} \sum_{m=0}^{q-1} G(-p,m,q)\delta(s - \tfrac{2\pi k}{M} - \tfrac{2\pi m}{Mq})$$

The generalized quadratic Gauß sums are defined by

$$\sum_{l=0}^{|c|-1} e^{2\pi i(al^2+bl)/c},$$

for given integers a, b, c, with $c \neq 0$.

$$G(-p,m,q) = \begin{cases} \sqrt{q}e^{i\theta m}, & \text{if } q \text{ is odd,} \\ \sqrt{2q}e^{i\theta m}, & \text{if } q \text{ is even and } q/2 \equiv m \mod 2, \\ 0, & \text{if } q \text{ is even and } q/2 \not\equiv m \mod 2, \end{cases}$$

for a certain angle θ_m that depends on m (and, of course, on p and q, too).

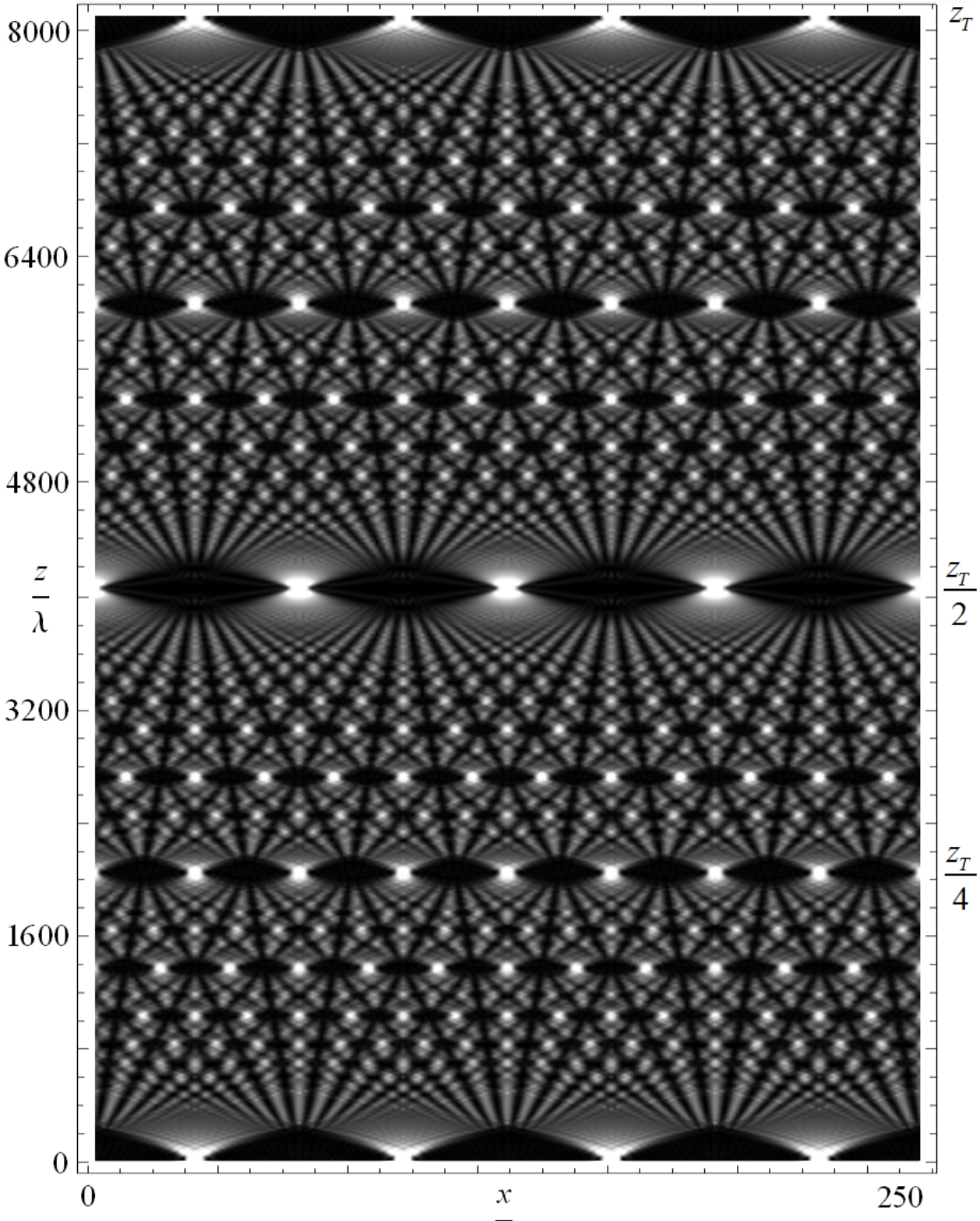
8000
6400
4800
$\frac{z}{\lambda}$
3200
1600
0
0
$\frac{x}{\lambda}$
250
z_T
$\frac{z_T}{2}$
$\frac{z_T}{4}$

Riemann's non-differentiable function

Integrating the Fourier series in time and evaluating at $x = 0$ we get

$$\phi(t) = i \int_0^t u(0,\tau)\, d\tau = \sum_{k\in\mathbb{Z}} \frac{e^{-4\pi^2 i k^2 t} - 1}{-4\pi^2 k^2},$$

which is essentially Riemann's non-differentiable function.

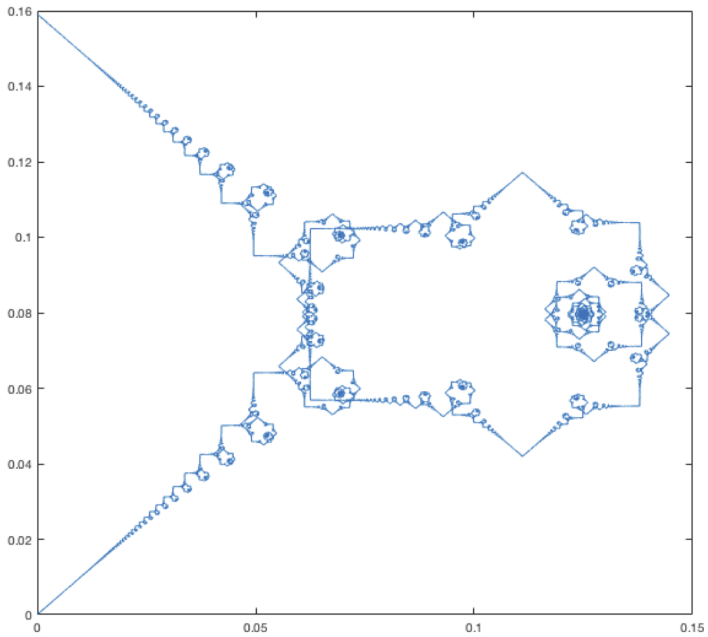

Figure: De la Hoz, Vega: *Vortex filament equation for a regular polygon*, Nonlinearity **27** (2014), 3031-3057

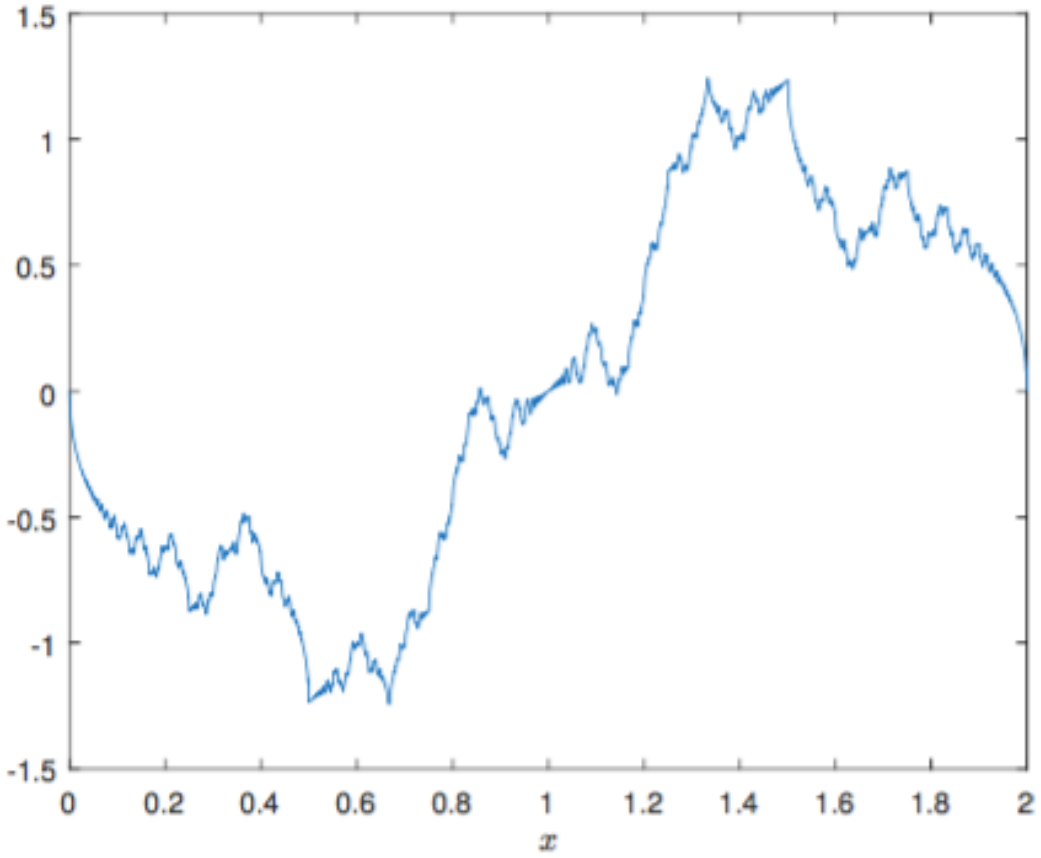
1.5
1
0.5
0
-0.5
-1
-1.5
0
0.2
0.4
0.6
0.8
1
1.2
1.4
1.6
1.8
2
x

$$\phi(t) = \sum_{k \neq 0} \frac{e^{\pi i k^2 t}}{i \pi k^2}, \quad t \in [0, 2]$$

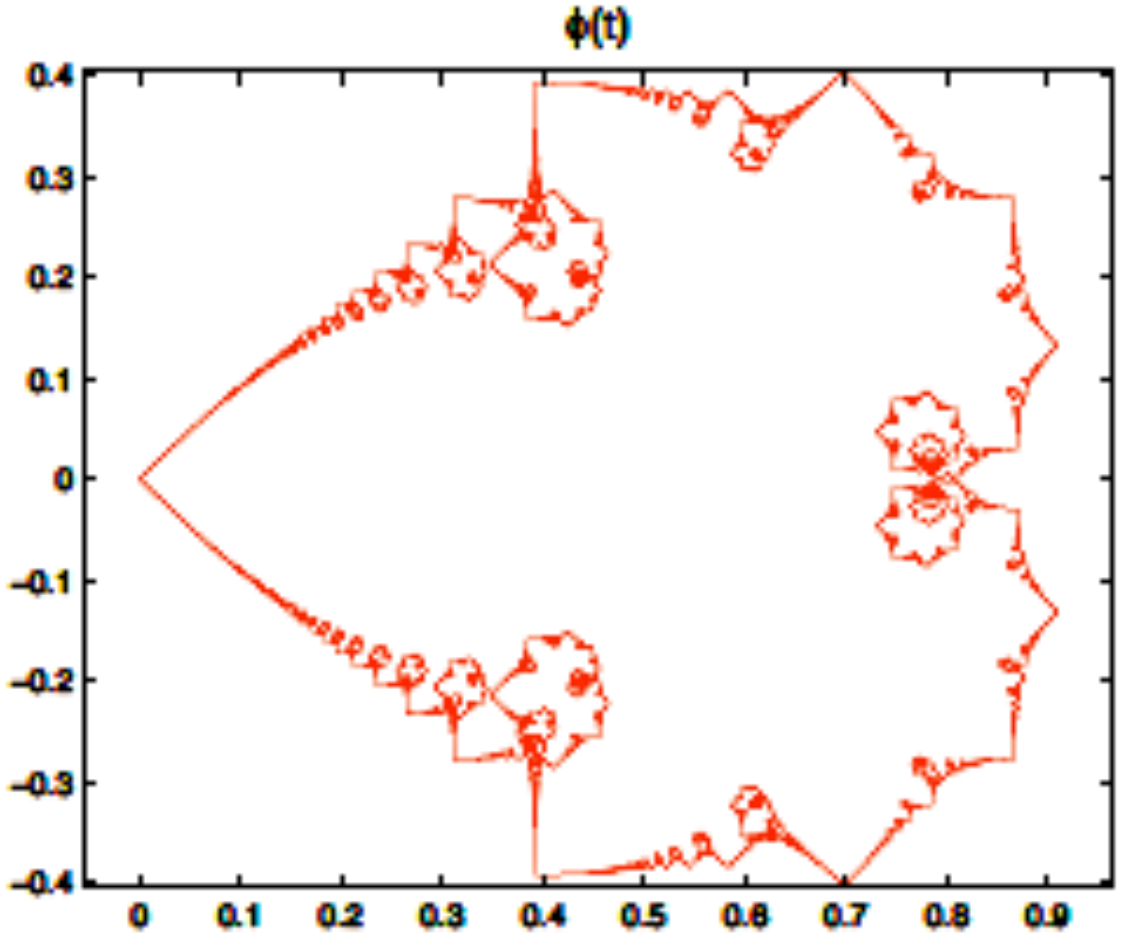

- Jaffard
- Multifractal (Frisch–Parisi conjecture)

- Berry and Goldberg, Talbot Effect '88,
- Duistermaat '91,
- Oskolkov '92,
- Jaffard, multifractal '96,
- Kapitanski, Rodnianski '99,
- Olver '10
- Chen-Olver '12 '14; Olver-Sheils '17 Olver-Tsatis '18
- Jerrard–Smets '15,
- Erdogan–Tzirakis '13,
- De la Hoz–Vega '13, '17 critical regularity,
- Banica–Vega '18 critical regularity.

A REGULAR POLYGON (w/ F. de la Hoz, NLTe)

$$\psi(s,0) = \frac{2\pi}{M} \sum_{k=-\infty}^{\infty} \delta\left(s - \frac{2\pi k}{M}\right).$$

- Galilean Transformations

$$\tilde{\psi}(s,t) \equiv e^{iks - ik^2 t}\psi(s - 2kt, t), \quad \forall\, k,t \in \mathbb{R}.$$

$$e^{2\pi i j M s}\psi(s,0) = \psi(s,0) \quad \forall\, j \in \mathbb{Z}.$$

$$\tilde{\psi}_k = \psi \quad \forall\, k \in \mathbb{Z}.$$

$$\widehat{\psi}(k,t) \quad = \quad e^{-i(Mk)^2 t}\widehat{\psi}(0,t)$$

THE TALBOT EFFECT

$$t_{pq} = (2\pi/M^2)(p/q)$$

$$\psi(s,0) = \frac{2\pi}{M} \sum_{k=-\infty}^{\infty} \delta(s - \tfrac{2\pi k}{M}).$$

$$\psi(s,t_{pq}) = \frac{2\pi}{Mq} \sum_{k=-\infty}^{\infty} \sum_{m=0}^{q-1} G(-p,m,q)\delta(s - \tfrac{2\pi k}{M} - \tfrac{2\pi m}{Mq})$$

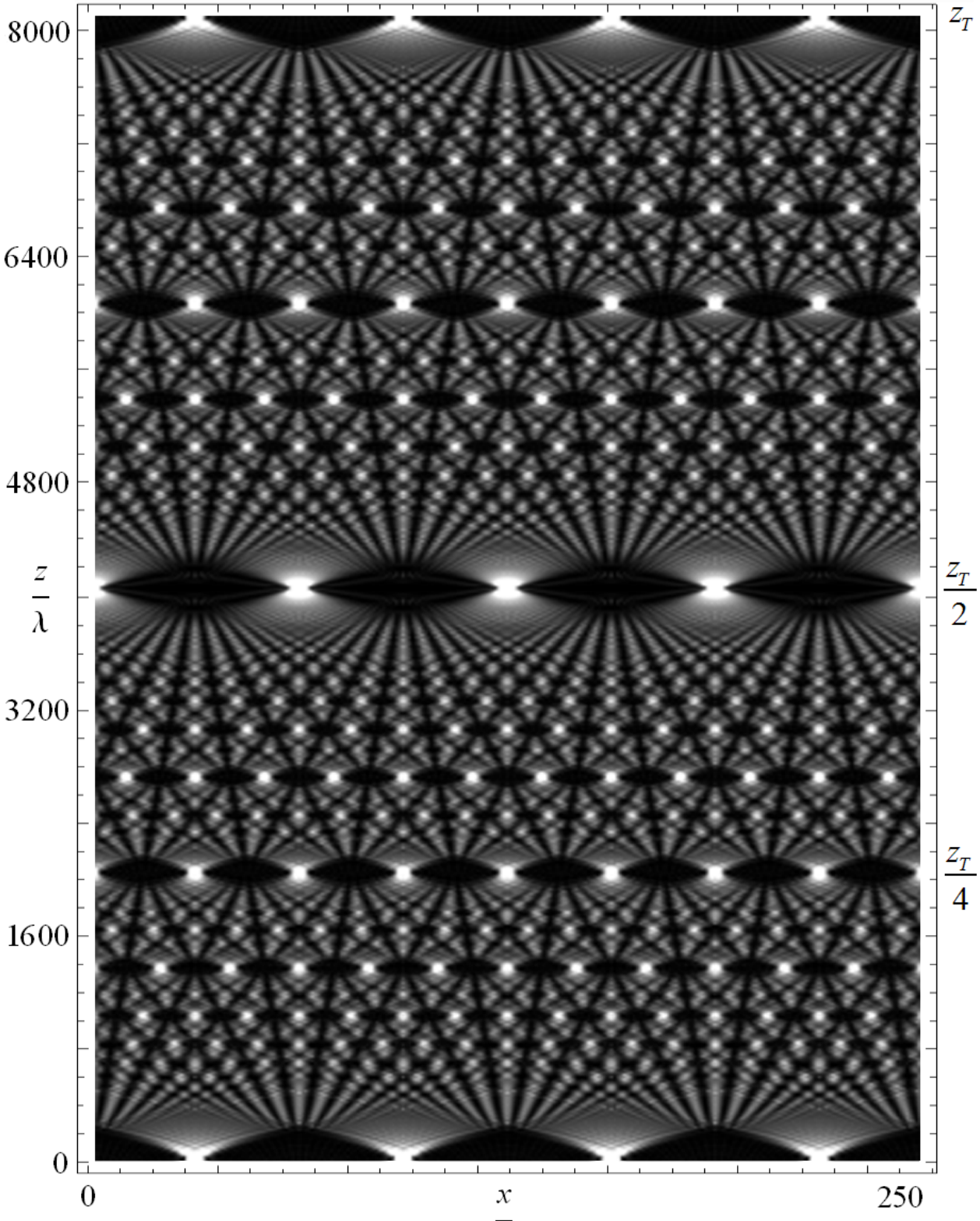
8000
6400
4800
$\frac{z}{\lambda}$
3200
1600
0
0
$\frac{x}{\lambda}$
250
z_T
$\frac{z_T}{2}$
$\frac{z_T}{4}$

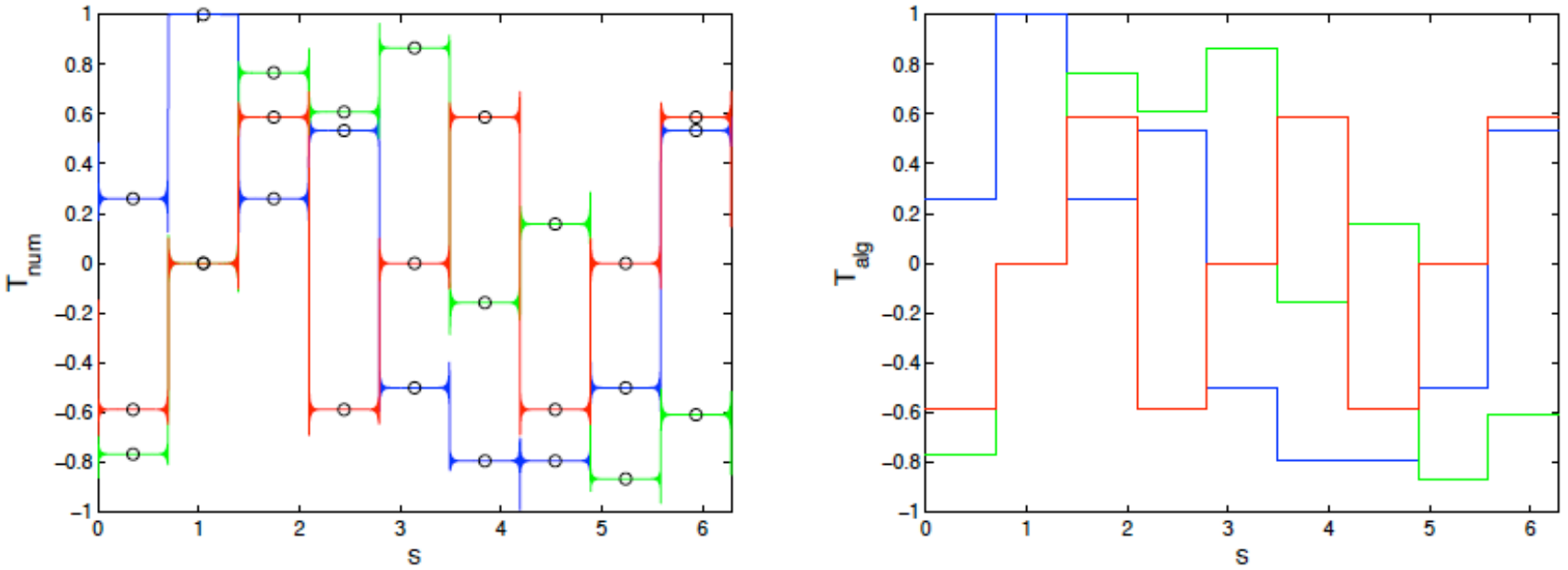

$\mathbf{T}_{num}$ versus $\mathbf{T}_{alg}$, for $M = 3$, at $T_{1,3} = \dfrac{2\pi}{27}$. T_1 appears in blue, T_2 in green, T_3 in red. In $\mathbf{T}_{num}$, the Gibbs phenomenon is clearly visible. The black circles denote the points chosen for the comparisons.

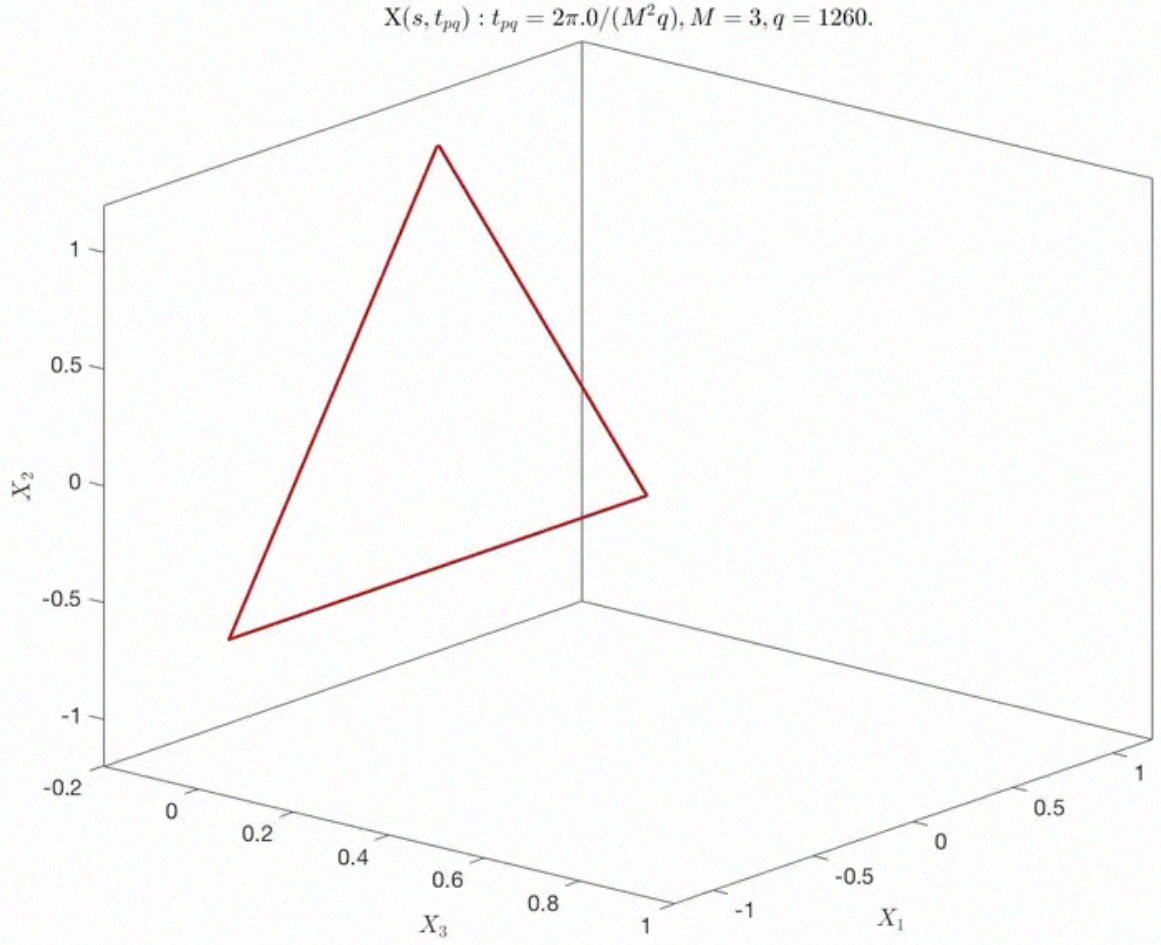
$\mathrm{X}(s, t_{pq}) : t_{pq} = 2\pi.0/(M^2 q), M = 3, q = 1260.$
1
0.5
0
-0.5
-1
X_2
-0.2
0
0.2
0.4
0.6
0.8
1
X_3
1
0.5
0
-0.5
-1
X_1

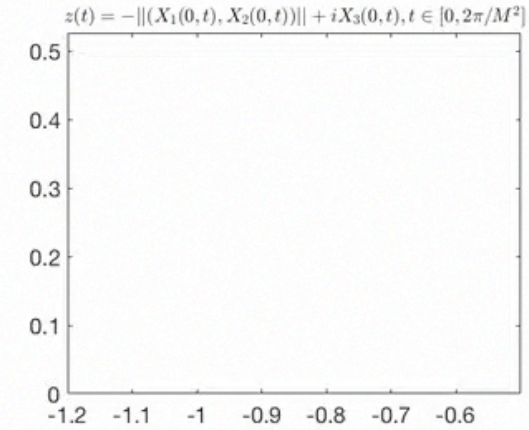
$z(t) = -||(X_1(0,t), X_2(0,t))|| + iX_3(0,t), t \in [0, 2\pi/M^2]$
0.5
0.4
0.3
0.2
0.1
0
-1.2
-1.1
-1
-0.9
-0.8
-0.7
-0.6

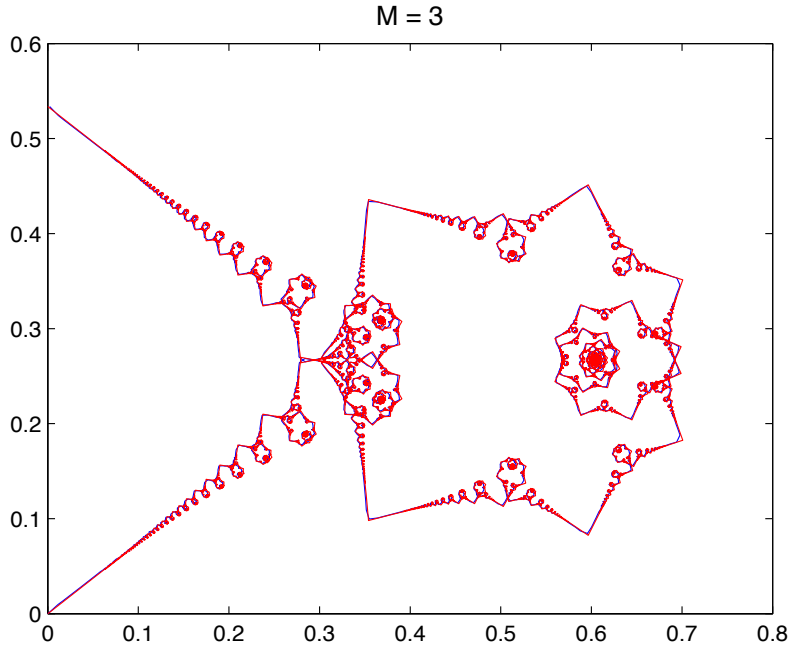
M = 3
0.6
0.5
0.4
0.3
0.2
0.1
0
0
0.1
0.2
0.3
0.4
0.5
0.6
0.7
0.8

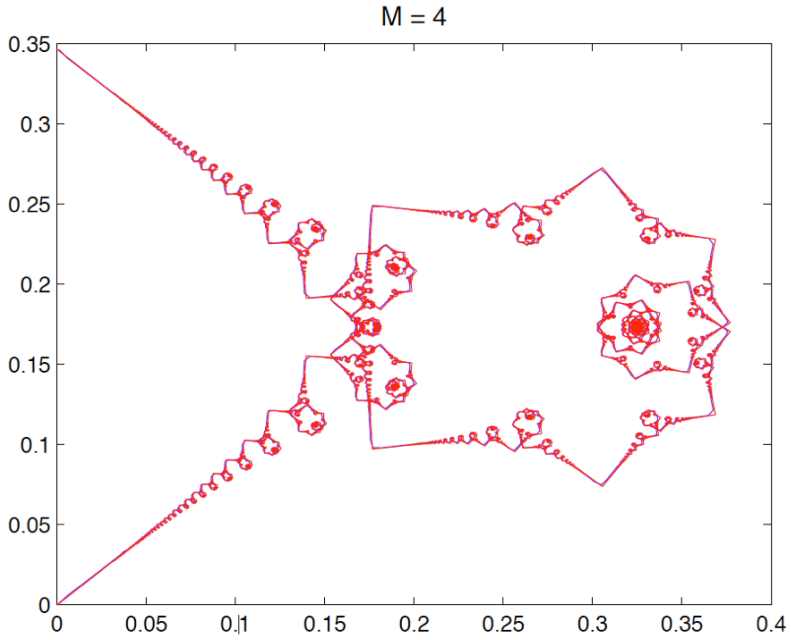
M = 4
0.35
0.3
0.25
0.2
0.15
0.1
0.05
0
0
0.05
0.1
0.15
0.2
0.25
0.3
0.35
0.4

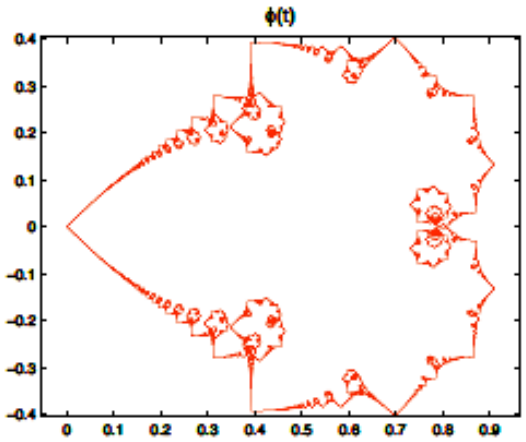
ϕ(t)

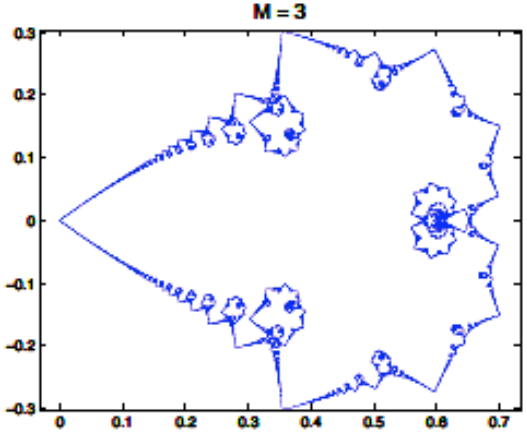
M = 3

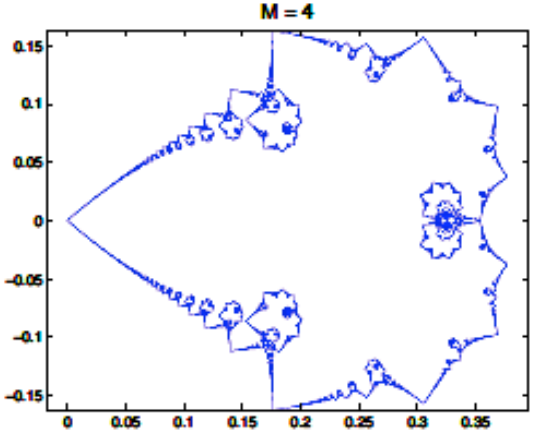
M = 4

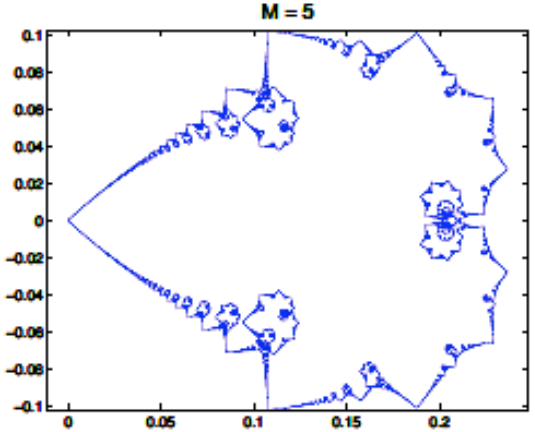
M = 5

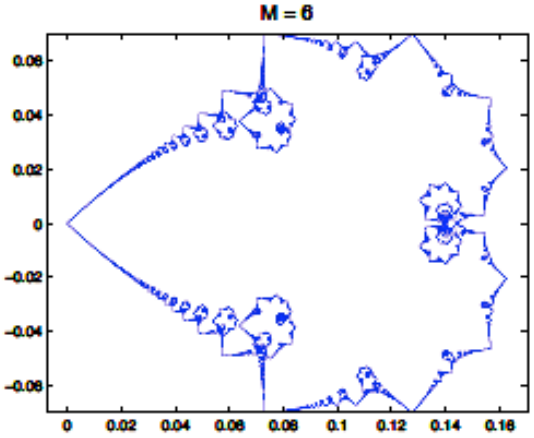
M = 6

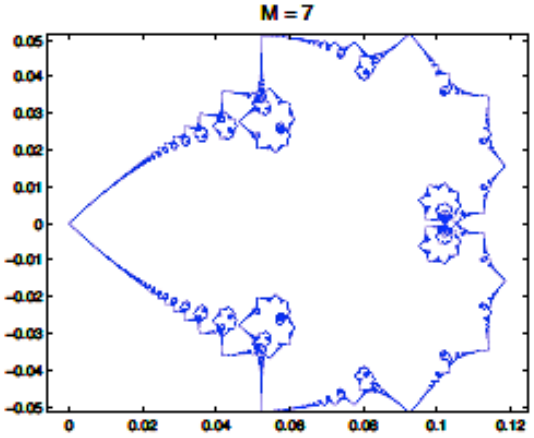
M = 7

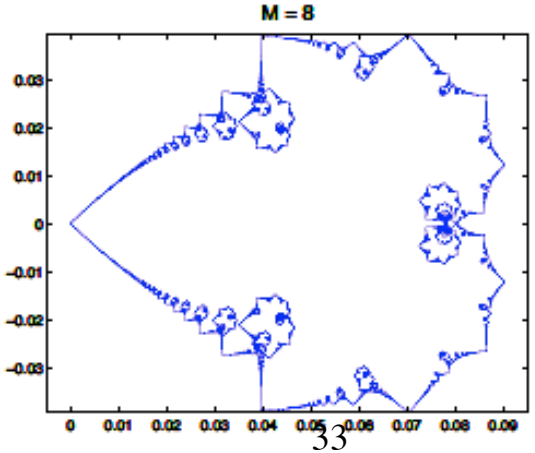
M = 8

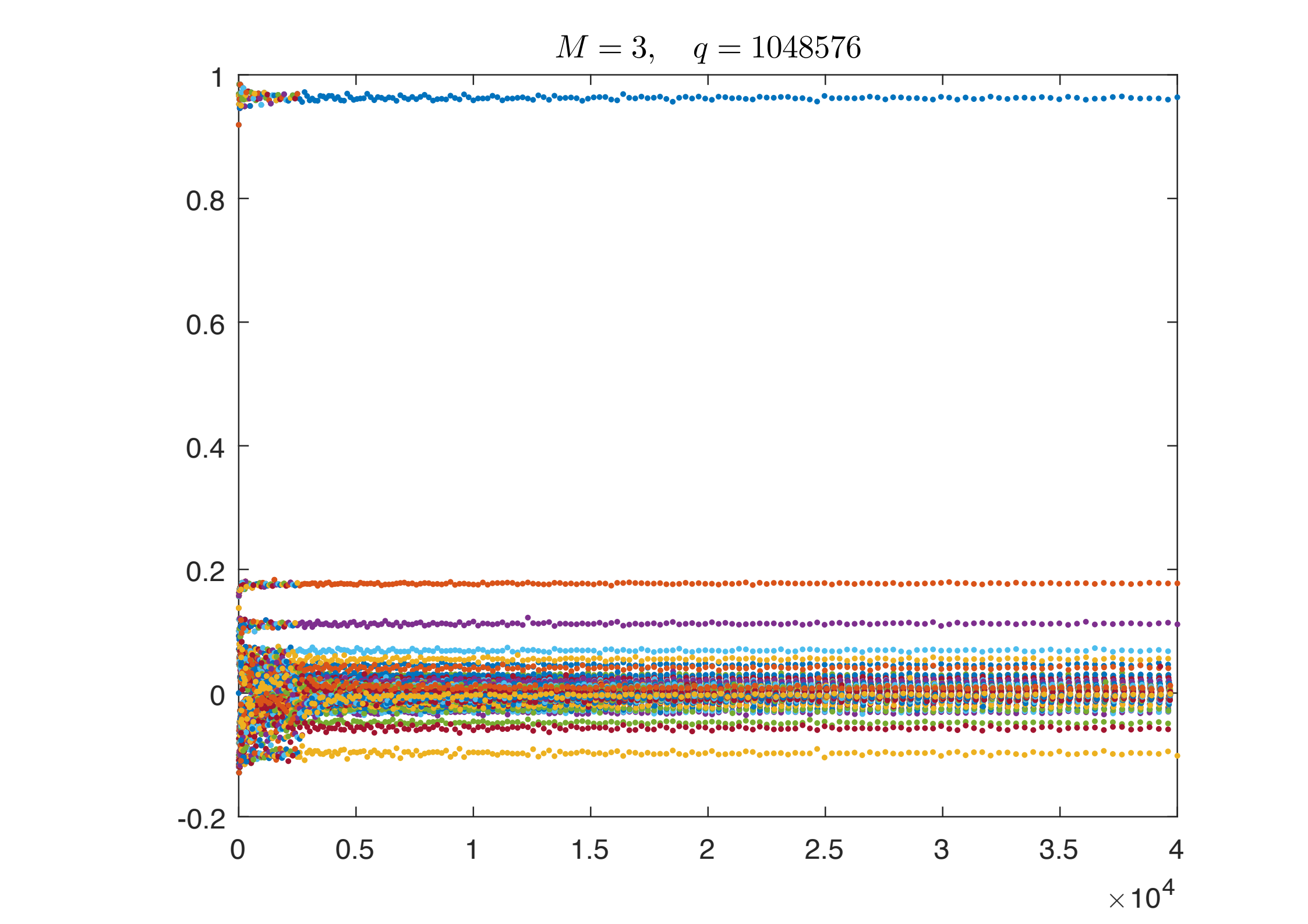
$M = 3, \quad q = 1048576$
1
0.8
0.6
0.4
0.2
0
-0.2
0
0.5
1
1.5
2
2.5
3
3.5
4
$\times 10^4$

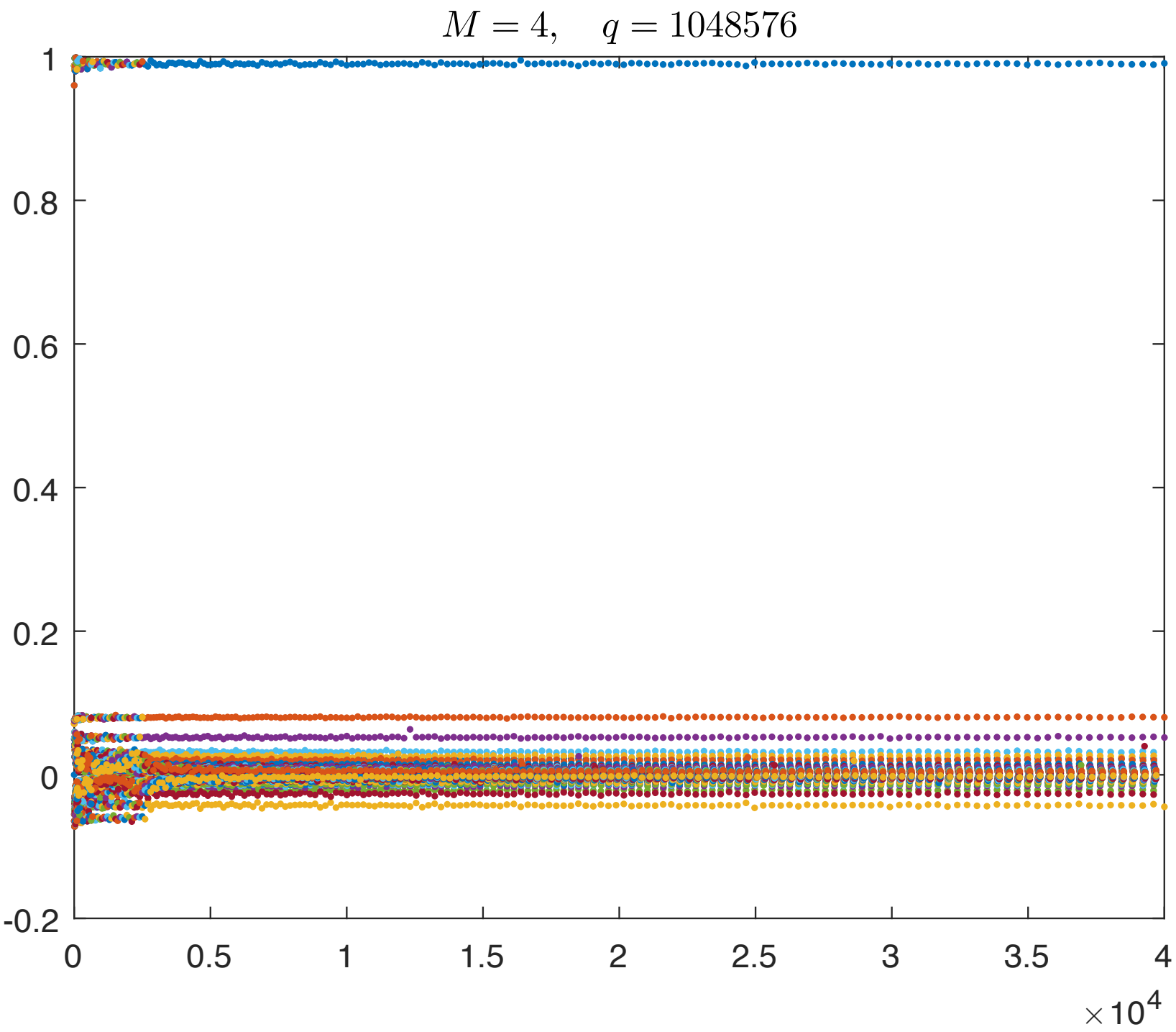
$M = 4, \quad q = 1048576$
1
0.8
0.6
0.4
0.2
0
-0.2
0
0.5
1
1.5
2
2.5
3
3.5
4
$\times 10^4$

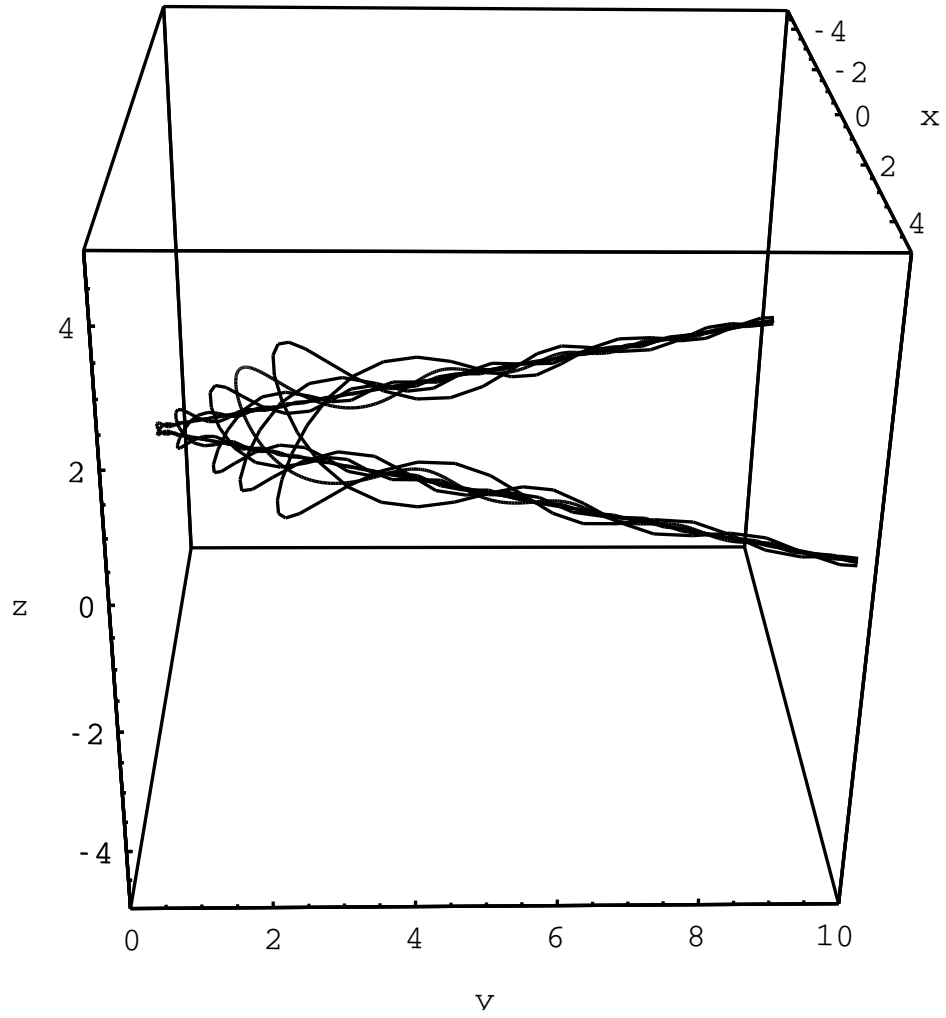

Theorem.– (with V. Banica) The self-similar solutions are stable. In particular, the creation/annilihation of a corner is stable.

Energy transfer

Theorem.– For $t > 0$ we have the following conservation law:

$$\|T(t)\|^2_{L^2_{sc}} = 4\pi \sum_j |a_j|^2,$$

but

$$(*) \qquad \|T(0)\|^2_{L^2_{sc}} = 4 \sum_j (1 - e^{-\pi |a_j|^2}),$$

where

$$\|T(t)\|^2_{L^2_{sc}} := \lim_{k \to \infty} \int_k^{k+1} |\widehat{T_s}(t, \xi)|^2 d\xi.$$

Energy Transfer, NLTe

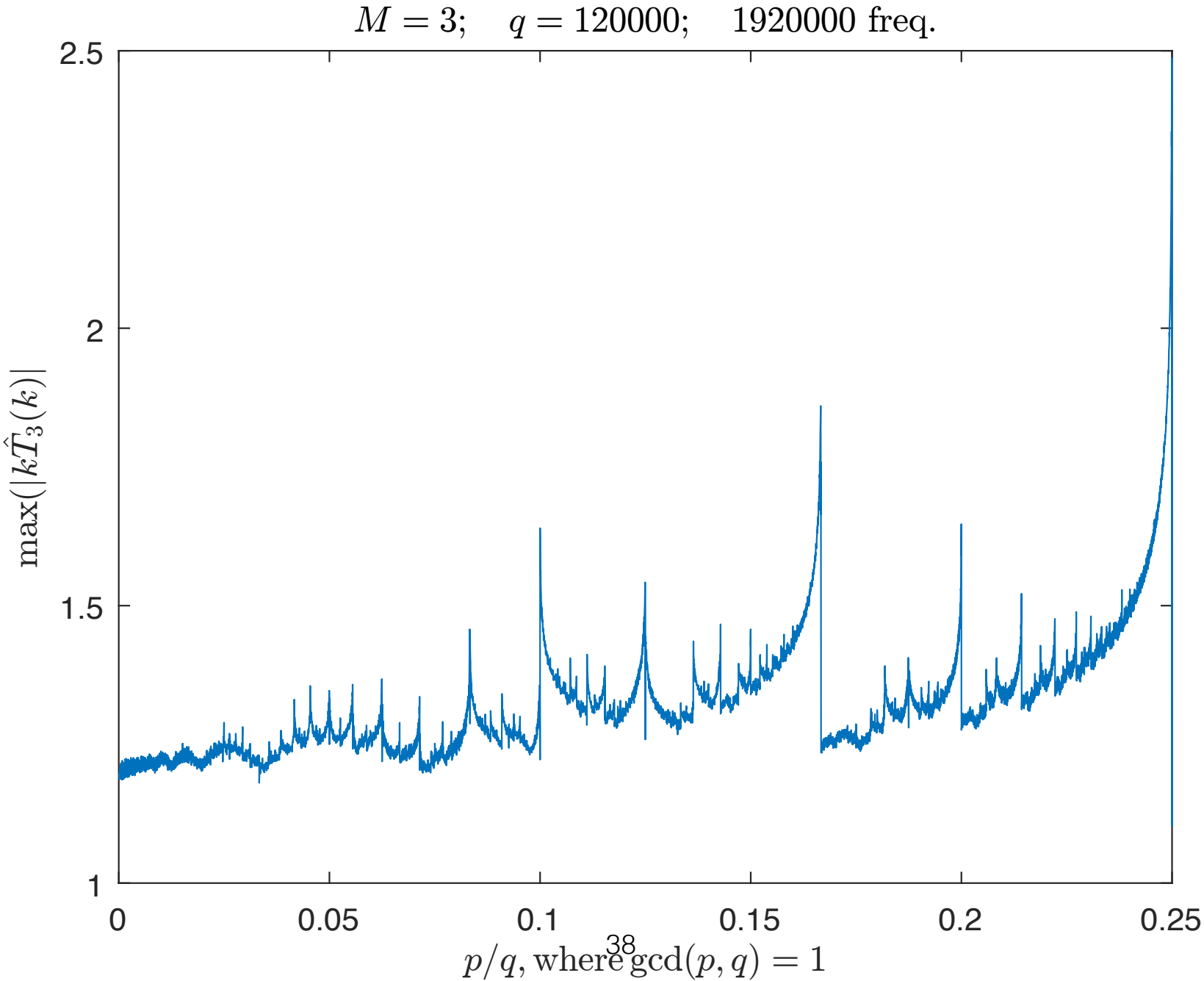

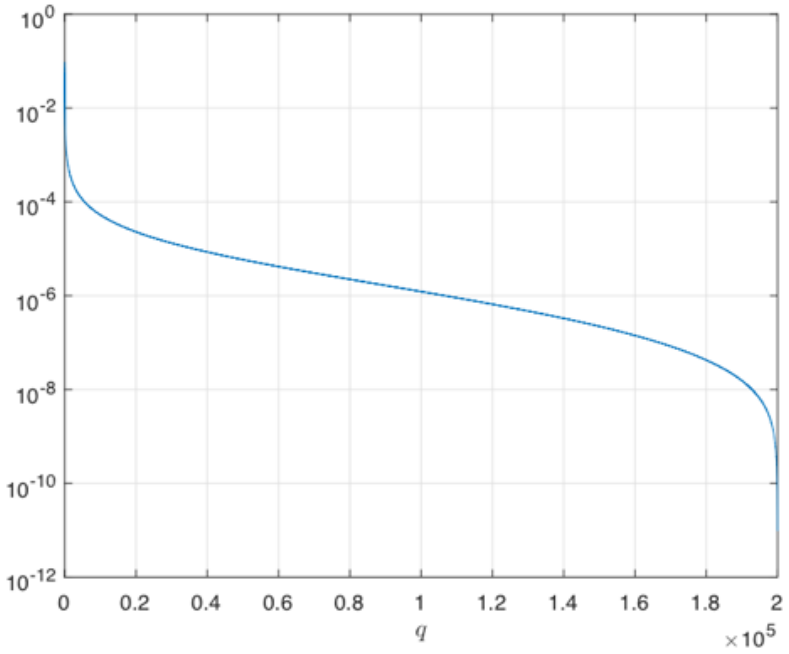

Figure 10: $|\sqrt{2}\max_{t_{pq}} \|\widehat{T_{1,s}}(t_{pq})\|_\infty - a\ln(q) - b|$, for $a = 0.258039752572419$, $b = 0.152992510344641$.